reactive and evolves gas rapidly upon reaction.

Standardization of the Me_2SO Solutions. To 5.0 mL of a known amount of 1.0 M HCl was added 1.0 M of the Me_2SO solution with cooling. The resulting aqueous solution was titrated to an end point with 1.5 M NaOH.

Preparation and Standardization of the Solutions of Methyllithium in THF. A two-necked, 100-mL, round-bottomed flask was fitted with a gas inlet adapter, a rubber septum, and a magnetic stirring bar. The gas inlet was attached to either aspirator or N_2. To this system was added 50 mL of CH_3Li in diethyl ether. The ether was then removed under reduced pressure. The system was opened to N_2, and 25 mL of dry THF was added by syringe. The system once again was placed under reduced pressure, and the THF was removed. The system was then again opened, and 25 mL of THF was added by syringe.

Standardization of the Solutions. To 5.0 mL of dry benzene in a two-necked, 100-mL, round-bottomed flask was added a small crystal of 1,10-phenanthroline. One neck of the flask was fitted with a septum, and N_2 was brought in through a needle. In the second neck was placed a septum, through which was placed a buret containing 1.0 mL of *sec*-butyl alcohol in xylene. To the benzene was added 1.0 mL of the MeLi-THF solution. The *sec*-butyl alcohol was then used to titrate the solution to an end point.

(Phenylsulfonyl)acetic acid was prepared by the method of Pasto and co-workers.[16] The resulting solid was recrystallized in hexane: mp 109-111 °C (lit.[16] mp 113-114 °C); yield 40%, IR 1725, 1325, 1245, 1150 cm^{-1}.

Ethyl 3-oxo-4-phenylbutanoate was prepared by the procedure of Kiang et al.[17] The compound was purified with a silica gel column and $CHCl_3$ as the mobile phase: R_f 0.8; yield 27.8 g (47%); NMR ($DCCl_3$) δ 7.24 (s, 5, arom), 4.17 (q, 2, CH_2O), 3.83 (s, 2, $COCH_2CO$), 3.41 (s, 2, $PhCH_2CO$), 1.20 (t, 3, CH_3); IR 2980 (m), 1740 (s), 1715 (s) cm^{-1}.

Registry No. **1**, dianion, 67157-48-6; **2**, dianion, 67157-44-2; **3**, dianion, 67157-50-0; **4**, dianion, 67157-49-7; **5**, dianion, 57557-41-2; **6**, dianion, 67157-45-3; **7**, dianion, 67157-47-5; **8**, dianion, 67157-46-4; **9**, dianion, 83026-88-4.

(16) Pasto, D. J.; McMillan, D.; Murphy, T. *J. Org. Chem.* **1965**, *30*, 2688-2691.
(17) Kiang, A. K.; Mann, F. G.; Prior, A. F.; Topham, A. *J. Chem. Soc.* **1956**, 1319-1331.
(18) St. Amour, T. E.; Burgar, M. I.; Valentine, B.; Fiat, D. *J. Am. Chem. Soc.* **1981**, *103*, 1128-1136.

Polymer Films on Electrodes. 10. Electrochemical Behavior of Solution Species at Nafion-Tetrathiafulvalenium Bromide Polymers

Timothy P. Henning, Henry S. White, and Allen J. Bard*

Contribution from the Department of Chemistry, University of Texas, Austin, Texas 78712.
Received February 19, 1982

Abstract: The electrochemical behavior of solution species at electrodes consisting of a conductive polymer layer, produced by incorporation of tetrathiafulvalenium (TTF^+) bromide into the cation-exchange polymer Nafion, on various substrates (Pt, Ta, SnO_2, n-Si) is described. The voltammetric behavior of the solution species $Fe(CN)_6^{3-}$ and FeY^{2-} (where Y^{4-} = ethylenediaminetetraacetate) at the Nafion-TTF^+ electrodes was consistent with models of electrodes partially covered with electronically conductive sites. Microscopic investigation of the electrode showed that the incorporated TTF^+ forms electroactive domains and conductive nonelectroactive crystals from electrochemical cycling. The nonelectroactive crystals have the same stoichiometry as the one-dimensional organic conductor $TTFBr_{0.7}$. In the electrodeposition of copper onto the TTF^+ polymer electrode, most deposited on the $TTFBr_{0.7}$, indicating that they were the major source of electronic conduction within the polymer. When the TTF^+ polymer was applied to the surface of an n-type Si electrode, the lifetime of the semiconductor electrode for the photooxidation of Fe(II) species was improved.

Polymer electrodes consist of thin (~0.1-10 μm) polymer layers on conductive (metal or carbon) substrates.[1-3] These include polymers containing electroactive groups in the polymer backbone and polyelectrolyte layers in which electroactive ions are held by electrostatic binding.[2] In these materials charge is transported by diffusion and migration of the ions as well as by electron hopping between electroactive sites. Electronically conductive polymers[3] and the related one-dimensional organic metals[4] (e.g., TTF-TCNQ, where TTF is tetrathiafulvalene and TCNQ is

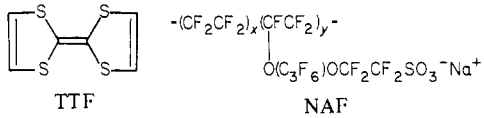

TTF NAF

tetracyanoquinodimethane) have also been employed as electrodes. We recently described a polymer electrode in which tetrathiafulvalenium (TTF^+) was incorporated into a layer of the perfluorinated sulfonate polymer Nafion (NAF) and proposed that charge transfer through this layer occurred by both electronic and ionic conduction (i.e., was a "biconductive" polymer layer).[5] The evidence for this electronic conductivity with incorporated TTF^+ was the significantly higher charge transfer through this layer compared to that of Nafion layers containing other ions, such as $Ru(bpy)_3^{2+}$. In this paper we describe more detailed studies of

(1) (a) Merz, A.; Bard, A. J. *J. Am. Chem. Soc.* **1978**, *100*, 3222. (b) Itaya, K.; Bard, A. J. *Anal. Chem.* **1978**, *50*, 1487. (c) Van De Mark, M. R.; Miller, L. L. *J. Am. Chem. Soc.* **1978**, *100*, 639. (d) Daum, P.; Murray, R. W. *J. Electrochem. Soc.* **1979**, *103*, 289. (e) Kaufman, F. B.; Engler, E. M. *J. Am. Chem. Soc.* **1979**, *101*, 547.
(2) (a) Oyama, N.; Anson, F. C. *J. Electrochem. Soc.* **1980**, *127*, 247. (b) *Ibid.* **1980**, *112*, 271. (c) Rubinstein, I.; Bard, A. J. *J. Am. Chem. Soc.* **1980**, *102*, 6641. (d) *Ibid.* **1981**, *103*, 5007. (e) Oyama, N.; Anson, F. C. *Anal. Chem.* **1980**, *52*, 1192.
(3) (a) Diaz, A. F.; Kanazawa, K. K. *J. Chem. Soc., Chem. Commun.* **1979**, 635. (b) Kanazawa, K. K.; Diaz, A. F.; Geiss, R. H.; Gill, W. P.; Kwak, J. F.; Logan, J. A.; Rabolt, J. F.; Street, G. B. *Ibid.* **1979**, 854. (c) Diaz, A. F.; Castillo, J. I. *Ibid.* **1980**, 397. (d) Kanazawa, K. K.; Diaz, A. F.; Gill, W. D.; Grant, P. M.; Street, G. B.; Gardini, G. P. *Synth. Met.* **1979/1980**, *1*, 329. (e) Bull, R. A.; Fan, F. R.; Bard, A. J. *J. Electrochem. Soc.* **1982**, *129*, 1009.
(4) (a) Jaeger, C. D.; Bard, A. J. *J. Am. Chem. Soc.* **1979**, *101*, 1690. (b) *Ibid.* **1980**, *102*, 5435.
(5) Henning, T. P.; White, H. S.; Bard, A. J. *J. Am. Chem. Soc.* **1981**, *103*, 3937.

0002-7863/82/1504-5862$01.25/0

the electrochemical behavior of solution redox couples on the Nafion–TTF^+ electrode and microscopic examinations of the electrodes. These studies provide further evidence of electronically conductive domains in the layer as well as electrode behavior consistent with a surface of electroactive sites distributed across a nonconductive substrate. In a companion paper we discuss the electrochemical behavior of the TTF,NAF layer itself.[6]

Experimental Section

Materials. TTF (Aldrich) was purified by several vacuum sublimations. TTFCl was synthesized by dissolving TTF in benzene and adding dropwise a benzene solution that was saturated with chlorine. The resulting purple TTFCl precipitate was washed with ether and air-dried. FeY^{2-} (where Y^{4-} is ethylenediaminetetraacetate) and prepared by dissolving the potassium salt of EDTA in a thoroughly deaerated aqueous solution (pH 7) and adding $Fe(NH_4)_2(SO_4)_2$. The 970 equiv wt NAF dissolved in ethanol as a 2% solution was a gift from Du Pont.

Apparatus. All electrochemical experiments were done with a Princeton Applied Research Model 175 universal programmer, 173 potentiostat, and 179 digital coulometer. Current–time curves were recorded on a Norland Model 3001 digital oscilloscope or an x–y recorder. Rotating disk measurements were done with a Pine Instruments ASR-2 rotator and a Pine Instruments rotating ring disk electrode (disk area 0.458 cm^2). Electron micrographs were recorded on a JEOL JSM 35-C electron microprobe analyzer. Optial micrographs were made with a Zeiss IM-35 inverted microscope, using an Olympus OM-2 camera and Kodak Ektachrome 160 tungsten corrected film. The working electrode used in voltammetric experiments was a Pt disk (electrode area 0.027 cm^2) embedded in a glass rod. Tantalum electrodes were fabricated by sealing a Ta wire in glass and using the exposed cross section of the end of the wire as an electrode (electrode area, 0.049 mm^2). SnO_2 glass electrodes were prepared by attaching a Cu wire to the conducting SnO_2 surface using silver paint and covering the contact with a nonconducting epoxy. Contact was made to the backside of an n-Si single crystal with In–Ga amalgam. The exposed surface was etched with HNO_3:HF:HOAc (3:3:1) for 15 s, rinsed with EtOH, and air-dried before use. A Pt mesh was used as counterelectrode and a saturated calomel electrode (SCE) as a reference electrode in all experiments.

Procedure. The electrodes were prepared by covering the conductive substrate (Pt, Ta, Si, SnO_2) with 10 μL of a 2% by weight Nafion/EtOH solution and allowing the EtOH to evaporate. The dry thickness of the resulting films, as determined with a Sloan Dektak surface profile measuring system, were typically ~ 1 μm. The TTF^+ was incorporated into the film by immersing the electrode in an aqueous solution of 1 mM TTFCl for 10 min. The electrode, denoted substrate/NAF,TTF^+, turned a golden color after immersion in the TTF^+ solution, indicating the incorporation of TTF^+. The concentration of electroactive TTF^+ in the polymers as determined by integrated steady-state reductive charge in cyclic voltammetry was typically 0.3 M.

Results

Electrochemistry of Solution Species at NAF,TTF^+ Electrodes. The initial reduction of a freshly prepared Pt/NAF,TTF^+ electrode in 1.0 M KBr, when studied by cyclic voltammetry (CV), produced a broad cathodic wave similar to waves observed for other electroactive molecules incorporpated into Nafion polymer layers.[2c,d] The subsequent oxidation and reduction waves, however, were sharp peaks separated by ~ 150 mV (Figure 1a). Similar cyclic voltammograms were observed with KI and KCl as supporting electrolytes with the only significant difference being a shift in the peak potentials of both the reduction (E_{pc}) and oxidation (E_{pa}) waves with the different electrolytes. The Pt/NAF,TTF^+ electrode, which was originally golden in color, became colorless when the film was reduced in KBr and then purple when the film was reoxidized. The electrode was stable under constant electrochemical cycling between these peaks at 10 mV/s for several hours. The behavior of solid films of TTF on Pt substrates formed by evaporating a benzene solution containing dissolved TTF has been described.[5] The remarkable similarities between the cyclic voltammograms of the Pt/TTF and Pt/NAF,TTF^+ electrodes demonstrated that the behavior of the TTF in the polymer was closer to that of a conductive solid phase rather than to a polymer-bound species. Details of the behavior of Pt/NAF,TTF^+ electrodes are given elsewhere.[6]

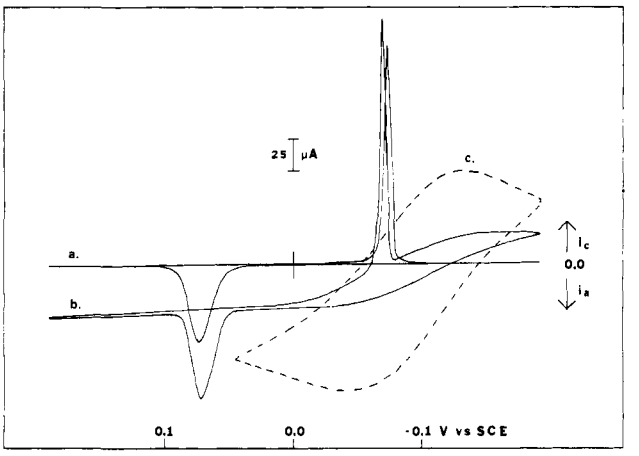

Figure 1. Cyclic voltammograms at 10 mV/s of (a) Pt/NAF,TTF^+ electrode in 1 M KBr, (b) Pt/NAF,TTF^+ electrode in 80 mM FeY^{2-}, 1 M KBr, (c) bare Pt electrode in 80 mM FeY^{2-}, 1 M KBr. Electrode area is 0.027 cm^2. Y^{4-} = $EDTA^{4-}$.

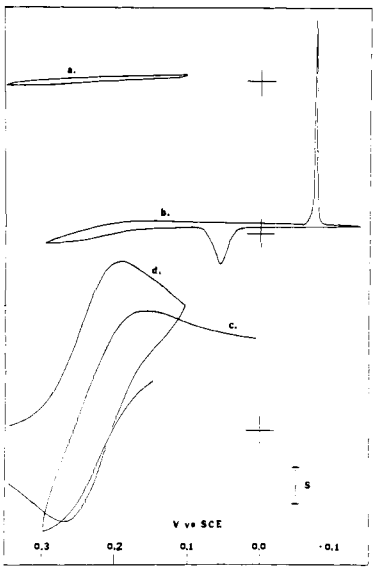

Figure 2. Cyclic voltammograms at 10 mV/s in 10 mM $Fe(CN)_6^{3-}$, 1 M KBr of (a) Pt/NAF electrode, S = 5 μA, (b) Pt/NAF,TTF^+ electrode, S = 50 μA, (c) As (b), at higher sensitivity, S = 5 μA, (d) bare Pt electrode, S = 5 A. Electrode area is 0.027 cm^2.

The behavior of solution redox couples was examined on Pt/NAF,TTF^+ electrodes to obtain further evidence concerning the conduction process in the films. The redox species chosen were large, highly charged anions. These anions were chosen for investigation because they did not readily permeate the cation-exchange polymer Nafion. Experiments at Pt electrodes covered with Nafion but containing no TTF^+ showed CV peak currents for the electrochemical reduction of ferricyanide or oxidation of FeY^{2-} 50 times smaller than those at a bare Pt electrode of the same area (Figure 2a). The steady-state cyclic voltammogram of a Pt/NAF,TTF^+ electrode in a ferricyanide solution is shown in Figure 2b,c. Although ferricyanide is capable of oxidizing the reduced form, TTF, in the polymer, the CV behavior did not result in the usual mediated electron-transfer waves, where the waves of the incorporated species are perturbed. Instead, the Pt/NAF,TTF^+ electrodes showed ferricyanide reduction and ferrocyanide oxidation waves that are similar to those at a bare Pt electrode (Figure 2c). The ferricyanide reduction peak was shifted to a potential 30 mV more negative than on bare Pt, and the peak current was 70% of that on bare Pt, at a scan rate, v, of 10 mV/s. The TTF oxidation and reduction waves were unaffected by the solution species. If the cell was open circuited with the electrode in the reduced form, the electrode spontaneously oxidized in the presence of ferricyanide, indicating that the TTF form was only

(6) Henning, T. P.; Bard, A. J. *J. Electrochem. Soc.*, submitted for publication.

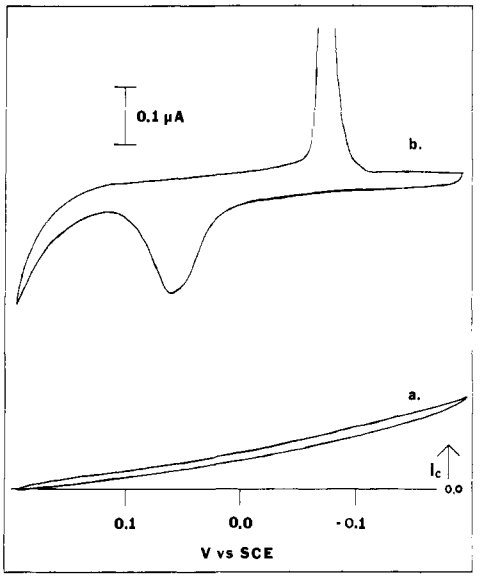

Figure 3. Cyclic voltammograms at 10 mV/s in 10 mM $Fe(CN)_6^{3-}$, 1 M KBr of (a) passivated Ta electrode, (b) Ta/NAF,TTF^+ electrode. Electrode area is 0.049 mm^2. Note that zero current level is the same for both (a) and (b).

stable under potential control. A similar study was carried out with another large, multiple-charged anion, FeY^{2-}. The CV of a Pt/NAF,TTF^+ electrode in these solutions is shown in Figure 1. FeY^{2-} is capable of reducing TTF^+, the oxidized form. However, again the electrode appeared to act as a conducting surface. Peak currents were 65% less than those seen at bare Pt, and the peak potentials were shifted 30 mV compared to those found at bare Pt. Thus, the results with FeY^{2-} again suggest that the Pt/NAF,TTF^+ electrode behaves as a conductive one.

Ta/NAF,TTF^+ Electrodes. The behavior of the solution redox species on Pt/NAF,TTF^+ electrodes might also be explained by pores or pinholes in the polymer layer that allow the solution species to reach the Pt substrate.[7] To demonstrate that this is not the case, experiments with a tantalum substrate were undertaken. Since Ta is readily passivated by formation of a nonconductive oxide,[8] any bare spots of a polymer coated Ta electrode would be blocked. A Ta electrode was passivated by scanning the electrode potential to 2.0 V in 1 M KBr. The CV of this passivated Ta electrode in a ferricyanide solution, shown in Figure 3a, shows that the reduction does not occur readily at the passivated Ta surface. The CV of a Ta/NAF,TTF^+ electrode (passivated at 2.0 V before coating with polymer) in 1 M KBr was similar to that with Pt substrates. The CV of a Ta/NAF,TTF^+ electrode in a ferricyanide solution is shown in Figure 3b. Note that all currents in Figure 3b are cathodic and the zero current axis is the same as that for Figure 3a. The ferricyanide reduction current at 0.1 V on the Ta/NAF,TTF^+ electrode was about 15 times larger than that at a bare Ta electrode and yielded a current density based on geometric area for ferricyanide reduction on Ta/NAF,TTF^+ electrodes approximately equal to that for Pt/NAF,TTF^+ electrodes. Thus the reduction of ferricyanide via pinholes in the NAF,TTF^+ layer is unlikely.

Chronoamperometric Experiments. The nature of the conductive surface of the Pt/NAF,TTF^+ electrode was investigated by potential step chronoamperometric investigation of ferricyanide reduction,[9] The electron potential was stepped from 0.35 V (where no appreciable reduction of the ferricyanide occurs and the electrode is in its oxidized form) to 0.0 V (well past the reduction peak of ferricyanide but not into the reduction wave of the TTF^+), and the current–time (i–t) trace was recorded. A

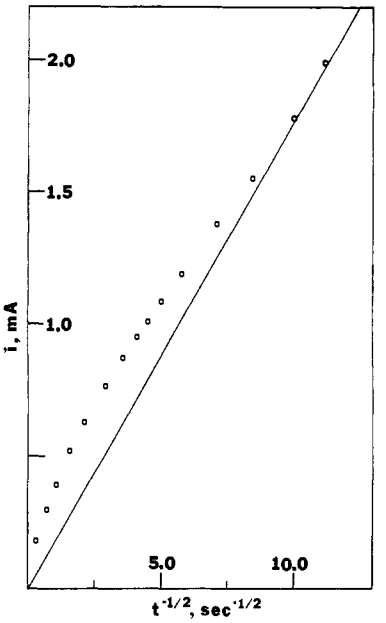

Figure 4. Plot of current vs. $t^{-1/2}$ for the reduction of ferricyanide on a Pt/NAF,TTF^+ electrode in a 10 mM $Fe(CN)_6^{3-}$, 1 M KBr solution. The potential was stepped from 0.35 to 0.0 V. Electrode area is 0.458 cm^2.

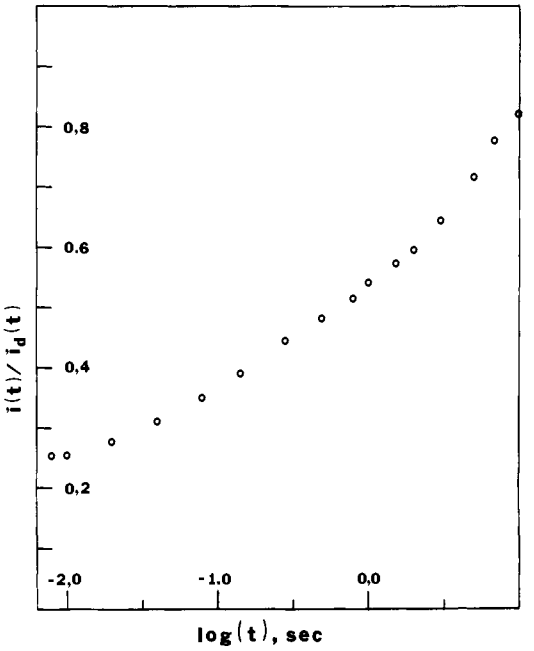

Figure 5. Plot of the ratio of currents observed at a Pt/NAF,TTF^+ electrode (i) and bare Pt electrode (i_d) vs. log t. Same experimental conditions as in Figure 4.

plot of i vs. $t^{-1/2}$ is shown in Figure 4. The current approached Cottrell behavior, a linear plot of i vs. $t^{-1/2}$ with zero itercept, at short times but deviated significantly from linear behavior at longer times ($t > 20$ ms). The behavior of the Pt/NAF,TTF^+ electrode can be compared to the response seen at a bare Pt electrode under the same experimental conditions, by plotting the dimensionless ratio of the current on the polymer-coated electrode to that of the bare electrode, i/i_d vs. log t (Figure 5),[7] At short times the ratio of the currents reached a constant value of 0.25, while at longer times the ratio of the currents increased. The short time limiting values depended on the loading of the polymers and were in the range of 0.1–0.35. The higher the initial concentration of TTF^+ introduced into the polymer, the larger was the value of the limiting ratio. The chronoamperometric results are consistent with an electrode surface composed of small conductive sites distributed across a nonelectroactive surface, as treated for

(7) Peerce, P. J.; Bard, A. J. *J. Electroanal. Chem.* **1980**, *112*, 97.
(8) Bard, A. J., Ed. "Encyclopedia of the Electrochemistry of the Elements"; Marcel Dekker: New York, 1974; Vol. 2, Chapter 3.
(9) Bard, A. J.; Faulkner, L. R. "Electrochemical Methods"; Wiley: New York, 1980; Chapter 5.

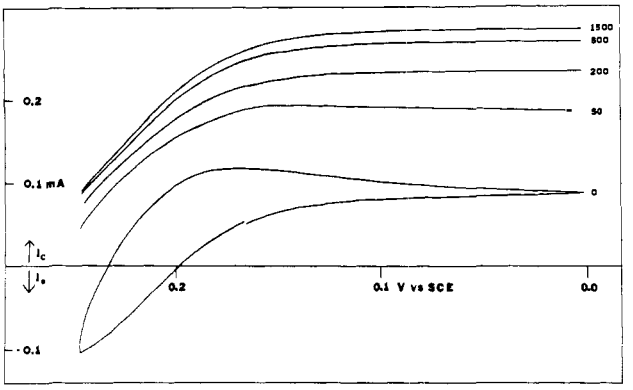

Figure 6. RDE voltammograms at 10 mV/s of a Pt/NAF,TTF$^+$ electrode in a 10 mM $Fe(CN)_6^{3-}$, 1 M KBr solution rotated at various speeds. Rotation rates are give in rpm. Electrode area is 0.458 cm^2.

chronoamperometric experiments by Gueshi et al.[10] These authors examined the electrochemistry of electrodes having uniformly distributed circular conducting sites across a surface, surrounded by hexagonal insulating regions. Although a similar geometry probably does not exist on Pt/NAF,TTF$^+$ electrodes, the limiting cases demonstrated by Gueshi et al. would generally be applicable. That is, at short times the diffusion layer will not have progressed very far from the conductive sites, and Cottrell behavior characteristic of the area of the electrochemically active sites is seen. As the diffusion layer for each conducting site grows out at longer times, the plot of i–$t^{1/2}$ deviaties from linearity. Eventually the diffusion zones overlap and Cottrell behavior characteristic of the total geometric area should occur. The current in Figure 4 approaches Cottrell behavior at short times but not at longer times. The dimensionless ratio of 0.25 obtained at short times (Figure 5) represents the ratio of the area of the electrochemically active sites to the geometric area of the electrode. The ratio steadily increases with time as expected, but the experiment was stopped before the limiting ratio of one was reached, Problems were encountered in these experiments with data collected at longer times, because of the onset of convection which caused deviations from semiinfinite linear diffusion. Although the rising portion of the curve shown in Figure 5 can be fit to working curves and estimates obtained for the radius of the conducting and nonconducting sites, the deviations of the surface geometry of the Pt/NAF,TTF$^+$ electrodes from that assumed in the theoretical model makes such values suspect.

Rotating Disk Experiments. Rotating disk electrode (RDE) voltammetry was used to investigate the reduction of ferricyanide on Pt/NAF,TTF$^+$ electrodes since such experiments can also provide information about the distribution of electroactive sites on electrode surfaces. Voltammograms for ferricyanide reduction at a Pt/NAF,TTF$^+$ electrode at several angular velocities (ω) are shown in Figure 6. The voltammograms at the Pt/NAF,TTF$^+$ RDE had the usual shape of RDE voltammograms on a metal surface. The limiting reduction current (i_l) decreased slowly with extended rotation times (e.g., during a 2-h experiment i_l decreased by ~10%). The CV TTF$^+$/TTF waves themselves also showed a more rapid decay for the rotated electrode compared to that in quiet solutions. A plot of the $1/i_l$ vs. $\omega^{-1/2}$ (Figure 7) is useful in characterizing the electrode surface. The data used in this plot were generated by holding the electrode at 0.0 V with the polymer in the oxidized form and varying ω. The Pt/NAF,TTF$^+$ electrode used to generate this plot was the same as that in Figures 4 and 5. Also shown in Figure 7 are data from a bare Pt electrode under the same conditions. The theory of electrolysis at partially covered rotating disk electrodes has been treated for different geometries of the conducting sites on the surface.[11] The surface geometry

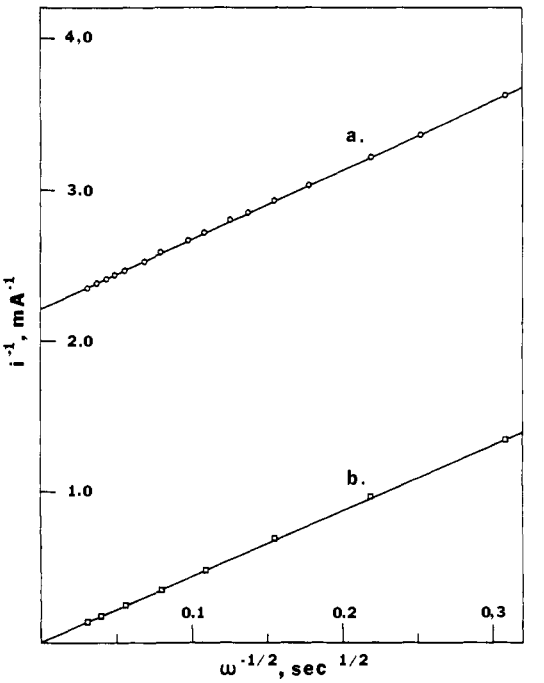

Figure 7. Plot of the reciprocal limiting current vs. the reciprocal square root of ω for the reduction of $Fe(CN)_6^{3-}$ on (a) Pt/NAF,TTF$^+$ electrode, (b) bare Pt electrode. The solution is 10 mM $Fe(CN)_6^{3-}$, 1 M KBr. Currents are recorded at 0.0 V. Electrode area is 0.458 cm^2.

Table I, Integrated Currents during Initial Cycling of Pt/NAF,TTF$^+$ Electrode in 1.0 M KBr

	Q, coulomb × 10^4	
cycle no.	cathodic	anodic
1	2.758	1.427
2	1.214	1.077
3	1.021	1,050
4	0.981	1.055
5	0.976	1.065

assumed in this model[11a] is similar to that used by Gueshi et al.[10] The theoretical and experimental studies of RDEs under these conditions show that $1/i_l$ varies linearly with $\omega^{-1/2}$ as long as the Nernst diffusion layer remains larger than one-half the spacing between the centers of the conducting circles. The slope of $1/i_l$ vs. $\omega^{-1/2}$ line is the same as that of a base electrode in the same solution. However, while a line for the bare electrode shows a zero intercept, that for the partially covered electrode has positive intercept whose magnitude depends on the size of the conducting sites on the electrode surface. However, while a line for the bare electrode shows a zero intercept, that for the partially covered electrode has positive intercept whose magnitude depends on the size of the conducting sites on the electrode surface. At sufficiently high rotation rates the Nernst diffusion layer becomes smaller than one-half the spacing between conducting sites, and the line deviates from linear behavior and approaches the line with a higher slope characteristic of the area of the conducting sites alone. The slope of the line for the rotated Pt/NAF,TTF$^+$ electrode (Figure 7) is the same as that for the bare Pt electrode up to the maximum rotation rate investigated (10^4 rpm). This suggests that the spacing between conducting sites must be less than ~10 μm.

Microscopic Investigation of Sub/NAF,TTF$^+$ Electrodes. The integrated charge under the CV waves of a Pt/NAF,TTF$^+$ electrode in a 1.0 M KBr solution (with no redox species in solution) decreased significantly on the initial scan and then more slowly through the first 4–5 cycles (Table I). After the first few cycles the CV waves were stable for several hours under continuous cycling. The material that was no longer electroactive did not go into solution but rather formed large crystals within the NAF matrix. This could be clearly seen in a scanning electron micrograph of the polymer surface exposed to the solution (Figure

(10) Gueshi, T.; Tokuda, K.; Matsuda, H. *J. Electroanal. Chem.* **1978**, *89*, 247.

(11) (a) Scheller, F.; Muller, S.; Landsberg, R.; Spitzer, H. *J. Electroanal. Chem.* **1968**, *19*, 187. (b) Scheller, F.; Landsberg, R.; Muller, S. *Ibid.* **1969**, *20*, 375. (c) Levart, E.; Schuhmann, D.; Contamin, O. *Ibid.* **1976**, *70*, 117.

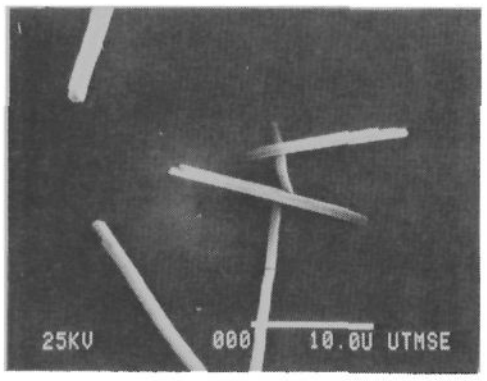

Figure 8. Scanning electrode micrograph of a Pt/NAF,TTF^+ electrode that has been electrochemically cycled 10 times in a 1 M KBr solution. Horizontal bar (bottom right corner) = 10 μm.

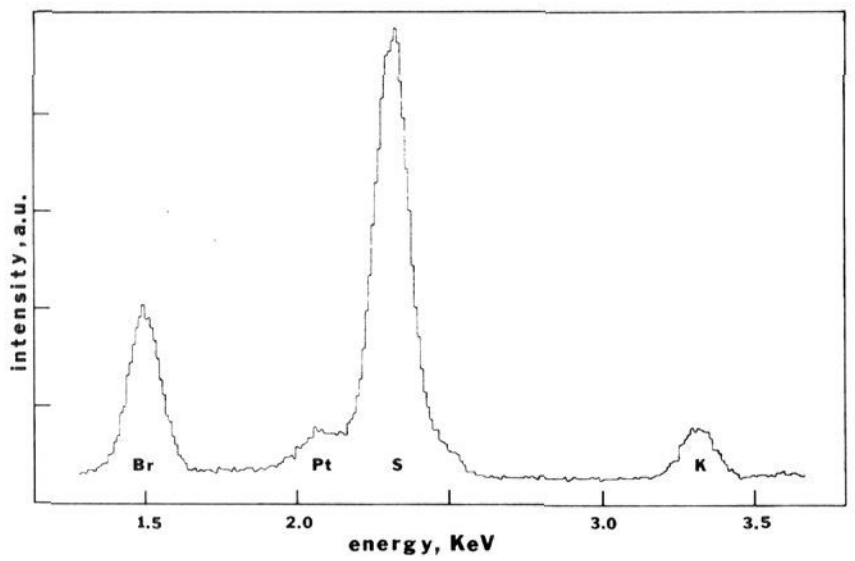

Figure 9. Energy dispersive spectrum of a crystal on the surface of a Pt/NAF,TTF^+ electrode (see Figure 8).

8). This Pt/NAF,TTF^+ electrode had been cycled in a 1.0 M KBr solution 10 times and was then removed from solution and the micrograph taken. A fresh Pt/NAF,TTF^+ electrode showed no crystals. The crystals evident on the surface were analyzed in the scanning electron microscope (SEM) by energy dispersive spectroscopy. The spectrum with the electron beam focused on a crystal is shown in Figure 9. The atomic ratio S/Br was 6.1 ($\pm$0.3)/1.0 ($\pm$0.2). The stoichiometry of the crystal, based on this ratio, is $TTFBr_{0.66\pm0.15}$. This stoichiometry is consistent with those reported for one-dimensional conducting crystals of TTF and Br, which show TTF/Br ratios of 1/(0.73–0.8).[12] The crystals were present on the electrode surface and appeared the same when the electrode was in either its oxidized or reduced state. While the SEM primarily provided information about the polymer surface, information about the total polymer structure was obtained by examining electrodes produced on transparent conductive substrates with an optical microscope. For those experiments a glass, conductive SnO_2/NAF,TTF^+ electrode was prepared; these showed electrochemical behavior very similar to those with a Pt substrate. Before electrochemical cycling, the SnO_2/NAF,TTF^+ electrode appeared homogeneous and uniform in color (golden to brown) and possessed no structure when examined at 400× magnification under the microscope. An electrode that had been electrochemically cycled several times in 1.0 M KBr and removed from solution in the oxidized form is shown in Figure 10a. The crystals present in the scanning electron micrograph were evident, but a structural change in other areas of the polymer had also occurred. Small ($\sim$1 μm) circular purple domains appeared throughout the electrode. For a SnO_2/NAF,TTF^+ electrode that was removed from solution in the reduced form (Figure 10b), large purple crystals were still present (these appeared the same for both the oxidized and reduced forms). However, the small circular purple domains present in the oxidized electrode disappeared when the electrode was in the reduced state. Thus two forms of TTF apparently are present in the electrochemically cycled polymer:

(12) Scott, B. A.; La Placa, S. J.; Torrance, J. B.; Silverman, B. D.; Welber, B. *J. Am. Chem. Soc.* **1977**, *99*, 6631.

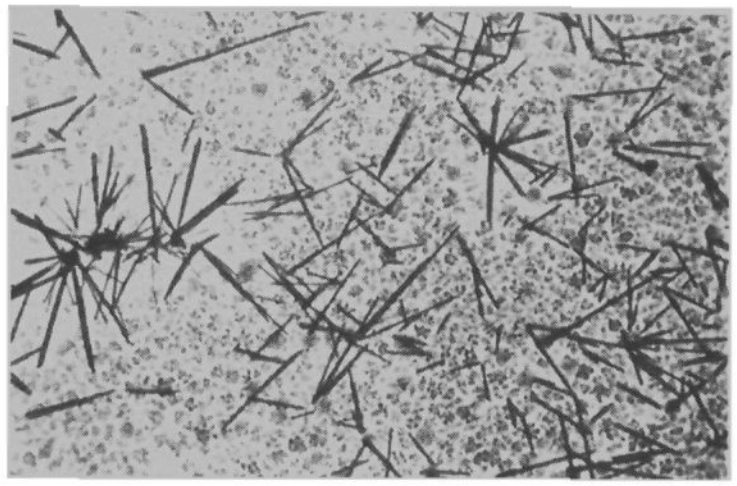

a.

50 μm

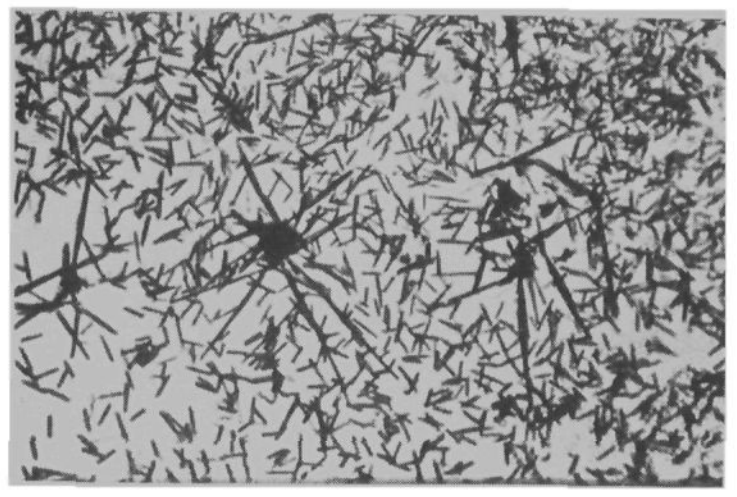

b.

Figure 10. Optical micrographs of SnO_2/NAF,TTF^+ electrodes that were cycled 10 times in a 1 M KBr solution and removed from solution in (a) the oxidized form, (b) the reduced form.

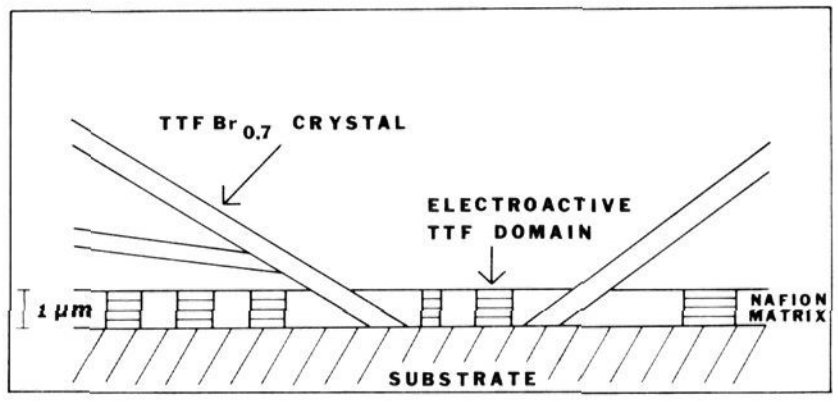

Figure 11. Diagram of the cross section of a Pt/NAF,TTF^+ electrode.

nonelectroactive crystals of $TTFBr_{0.7-0.8}$ and electroactive molecules of TTF distributed in small circular domains (Figure 11). From comparisons to the electrochemistry of solid films of TTF on conducting surfaces and the visible spectroscopic properties, we conclude that the oxidized form of the electroactive TTF is also of the composition $TTFBr_{0.7-0.8}$ and the reduced form is neutral TTF.[6]

The electrochemical reduction of ferricyanide at Pt/NAF,TTF^+ electrodes demonstrated the conductive nature of the polymer film but did not identify which sites were responsible for the conductivity. For more information about conductive sites on the electrode surface, the reduction of Cu^{2+} to metallic copper on a Pt/NAF,TTF^+ electrode in 1.0 M KBr solutions was carried out. A Pt/NAF,TTF^+ electrode was electrochemically cycled several times in 1.0 M KBr over the TTF^+/TTF waves. Then the negative limit of the scan was extended to –0.45 V and the scan stopped. Cupric bromide was added to the stirred solution (8.6 mM Cu^{2+}) and the deposition of Cu began immediately. The deposition was carried out for 5 min in the stirred solution before the electrode was removed. SEM examination of the electrode was performed by energy dispersive spectroscopy. Shown in Figure 12 are the spectra of a crystal and of a region adjacent to the crystal. The spectra were collected under conditions that the Pt peaks from

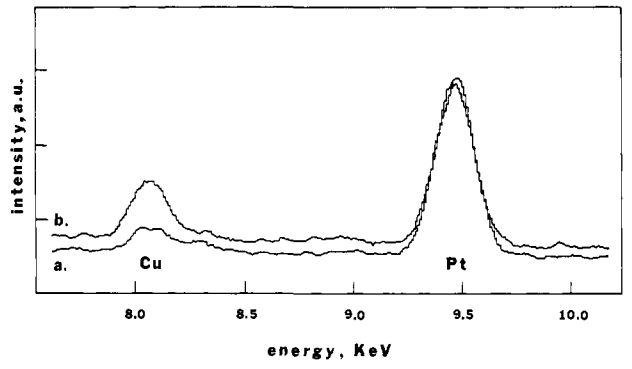

Figure 12. Energy dispersive spectra of a Pt/NAF,TTF^+ electrode that was subjected to copper deposition from an 8.6 mM $CuBr_2$, 1 M KBr solution. (a) Spectrum of electrode surface where no TTFBr crystals were present; (b) spectrum of a crystal on the electrode surface.

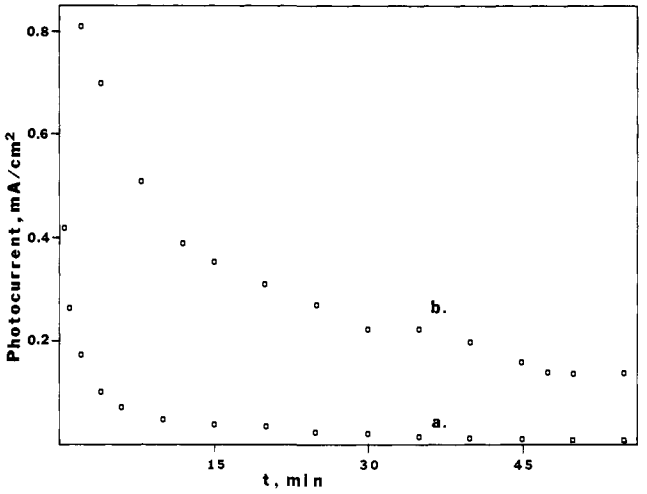

Figure 13. Photocurrent–time behavior of n-Si electrodes immersed in a stirred 0.1 M FeY^{2-}, 1.0 M KCl solution. (a) Bare n-Si; (b) n-Si/NAF,TTF^+. Illuminated with a 450-W Xenon lamp at $\lambda > 590$ nm. Focused power input ~ 150 mW/cm^2.

the substrate were of equal height. The region adjacent to the crystal showed a small Cu peak, presumably due to a small amount of Cu deposition at the small TTF^+ domains or on the Pt substrate by Cu(II) which diffuses through the polymer film. The Cu peak from a crystal was much higher than the background Cu peak. Thus the reduction of Cu^{2+} to Cu mainly occurs on the larger $TTFBr_{0.7}$ crystals in the polymer.

n-Si/NAF,TTF^+ Electrodes. One area of interest involving polymer films on electrodes is their use in protecting semiconductor electrode surfaces from photodecomposition.[13,14] Semiconductor electrodes have been widely investigated for possible applications in photoelectrochemical devices for the utilization of solar energy for the production of electricity or useful chemicals. However, many semiconductor electrodes tend to photocorrode under irradiation. For example, an n-type silicon (n-Si) electrode forms an insulating oxide film when illuminated in aqueous solutions. Consider an n-Si electrode immersed in an 0.1 M FeY^{2-} solution, held at a potential of −0.21 V vs. SCE ($\sim$150 mV positive of the flatband potential), and irradiated with a 450-W Xenon lamp (Figure 13a). The rapid decay of current during the photo-

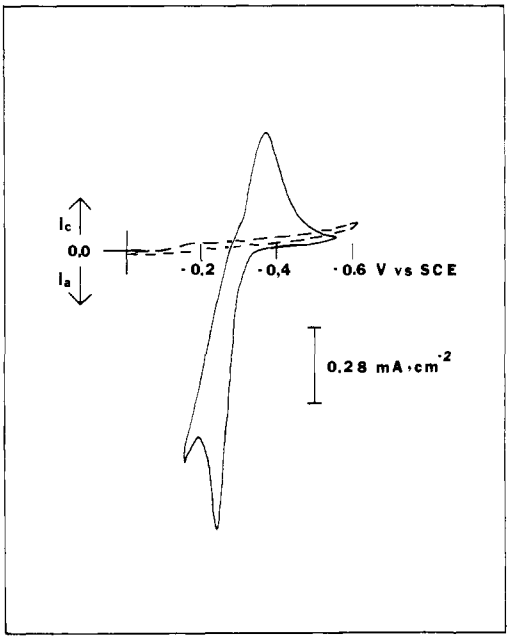

Figure 14. Cyclic voltammogram at 20 mV/s of an n-Si/NAF,TTF^+ electrode in a 1 M KCl solution. Electrode illuminated with a 450-W Xenon lamp at $\lambda > 590$ nm (—); electrode in the dark (--).

oxidation of FeY^{2+} results from oxide film formation. The electronically conductive polymer polypyrrole has been useful as a layer on n-Si to retard this photodecomposition.[13] Other polymers such as those containing electroactive groups on the polymer backbone have also been used with n-Si electrodes.[14] A key factor with such polymer layers is the rate of charge transfer through the film from the semiconductor surface to solution species, and the applicability of NAF/TTF^+ layers was investigated for this purpose.

The Nafion polymer was applied to the Si surface by the same methods as were used with Pt and Ta. The polymer did not adhere to the Si surface as well as it adhered to Pt, and in some experiments the polymer film peeled off of the Si surface. TTF^+ was incorporated into the polymer in the usual way. The CV from an n-Si/NAF,TTF^+ electrode immersed in 1.0 M KCl under irradiation and in the dark is shown in Figure 14. Photooxidation of the polymer film on the illuminated semiconductor and the corresponding reduction occurred in a sharp wave corresponding to thin-film behavior. The n-Si/NAF,TTF^+ electrode was cycled several times in solution and then placed in a stirred FeY^{2-} solution. The potential was held at −0.21 V vs. SCE and the photocurrent under Xenon lamp irradiation recorded (Figure 13b). Although the photocurrent decayed with time, the rate of decay was much slower than on the unprotected n-Si and the observed photocurrents were much higher. While the experimentally observed decay of the photocurrent at the polymer-coated semiconductor can be attributed in part to water penetration through the film and oxidation of the surface, other factors, such as loss of TTF^+ to the solution and peeling of the polymer from the Si, exposing bare surface, also contribute to the decay. These experimental results probably do not represent the best results that can be expected from this approach. By use of such strategies as thin metal undercoatings to promote better film adherence and high electrolyte concentrations to decrease water activity, as has been used with polypyrrole,[13a] better stability should result.

Discussion

The electrochemical and microscopic investigations lead to to the following model for the NAF/TTF^+ layer, the way it changes upon oxidative and reductive cycling, and the modes by which charge is transferred through it. The original Nafion layer, after incorporation of the TTF^+, is golden in color and represents TTF_2^{2+} contained in the hydrophilic sulfonate channels.[6] Upon reduction, the TTF remains within the polymer, probably in the

(13) (a) Fan, F. R.; Wheeler, B. L.; Bard, A. J.; Noufi, R. *J. Electrochem. Soc.* **1981**, *128*, 2042. (b) Noufi, R.; Frank, A. J.; Nozik, A. J. *J. Am. Chem. Soc.* **1981**, *103*, 1849. (c) Noufi, R.; Tench, D.; Warren, L. F. *J. Electrochem. Soc.* **1980**, *127*, 2310. (d) Skotheim, T.; Lundstorm, I.; Prejza, J. *J. Electrochem. Soc.* **1981**, *128*, 1625.

(14) (a) Wrighton, M. S.; Austin, R. G.; Bocarsly, A. B.; Bolts, J. M.; Hass, O.; Legg, K. D.; Wadjo, L.; Palazzotto, M. C. *J. Am. Chem. Soc.* **1978**, *100*, 1602. (b) Bolts, J. M.; Bocarsly, A. B.; Palazzotto, M. C.; Walton, E. G.; Lewis, N. S.; Wrighton, M. S. *Ibid.* **1979**, *101*, 1378. (c) Kubiak, C. P.; Schneemeyer, L. F.; Wrighton, M. S. *Ibid.* **1980**, *102*, 6898.

form of neutral TTF, and K^+ is introduced into the film. The subsequent oxidation causes introduction of Br^- into the film and probably the nucleation of $TTFBr_{0.7}$ structure. After a few cycles, some of these grow into the large needle crystals which are not electroactive and remain in the conductive $TTFBr_{0.7}$ form. This material is a known one-dimensional conductor.[11] The smaller zones, perhaps representing organized TTF^+Br^- structures within the Nafion channels, remain electroactive and account for the CV waves and color changes seen on cycling. Apparently these do not grow into crystals because of the hydrophobic zones surrounding them that are depleted of TTF^+.

The needle crystals are conductive and contact the substrate,[15] since electrodeposition of Cu was found on these. The spacing between these as observed by microscopy (~ 10 μm) is generally consistent with the spacings found in electrochemical measurements with analysis of the data according to the models for partially covered electrodes. Moreover, the RDE $1/i_l$ vs. $\omega^{-1/2}$ plots for reduction of ferricyanide show intercepts that are independent of whether the NAF,TTF film is in the oxidized or reduced state. This suggests that the overall area of conductive sites and their distribution are independent of the state of oxidation of the polymer film and point to the needle crystals as the conductive surface sites. The conduction within the small electroactive zones must also be rather rapid, however. The film redox processes show "thin-layer" behavior even at rather slow scan rates, under conditions where other species incorporated into Nafion (e.g., $Ru(bpy)_3^{2+}$) show "diffusion-controlled" behavior. While this might be ascribed to the effect of the needle crystals that penetrate the film acting as internal wires, the distance between these and the electroactive zones is of the order or larger of the film thickness itself. Thus we feel that there is also enhanced charge transfer within the electroactive zones. The major contribution to charge transfer to solution species reacting at the polymer film surface (e.g., $Fe(CN)_6^{3-}$) is probably made by the conductive needle crystals, however.

We might also contrast the behavior of these polymer films and those previously studied in which TTF was incorporated by covalent attachment to the polymer backbone.[16] While evidence of formation of TTF_2^{2+} species in the latter polymer was obtained, no crystallization or long-range ordering was observed, probably because of lesser flexibility in the chains and the absence of the organized channel structure which exists in Nafion.

Conclusions

The model of a biconductive polymer layer of Nafion with incorporated TTF species, in which both electronic and ionic conduction occurs, appears to be confirmed by these experiments. The electronic conduction to solution species takes place predominantly via μm-sized needle crystals of $TTFBr_{0.7}$. Separate electroactive TTF^+Br^- zones also exist in the film, however. Preliminary experiments suggest that these films might be useful as protective layers on semiconductor electrodes and perhaps might also be employed to incorporate catalysts onto electrode surfaces.

Acknowledgment. This research was supported by a grant from the National Science Foundation (CHE 7903729). The assistance of Dr. Michael Schmerling in obtaining the electron micrographs and of Cindy Williamson in obtaining the optical micrographs is gratefully acknowledged.

Registry No. NAF, 39464-59-0; TTF^+, 35079-56-2; Pt, 7440-06-4; Ta, 7440-25-7; SnO_2, 18282-10-5; Si, 7440-21-3; FeY^{2-}, 15651-72-6; TTF, 31366-25-3; KBr, 7758-02-3; ferricyanide, 13408-62-3; copper, 7440-50-8.

(15) The experiment shown in Figure 2b suggests that mediated charge transfer within the polymer layer between substrate and the crystals does not occur. Note that the net cathodic current on the far right ($E = -0.1$ V) is the same as that preceding the TTF^+ reduction peak. At these potentials only TTF in the neutral form is present, and mediated transport is unlikely.

(16) Kaufman, F. B.; Schroeder, A. H.; Engler, E. M.; Kramer, S. R.; Chambers, J. Q. *J. Am. Chem. Soc.* **1980**, *102*, 483.

Photochemistry in Polymerized Microemulsion Systems[1]

S. S. Atik and J. K. Thomas*

Contribution from the Chemistry Department, University of Notre Dame, Notre Dame, Indiana 46556. *Received December 28, 1981*

Abstract: The preparation of polymerized microemulsions, P-μE, by polymerization of a microemulsion consisting of cetyltrimethylammonium bromide, hexanol, styrene, and divinylbenzene is reported. Typically the P-μE are well defined and show radii in the range 200 to 400 Å. Unlike micelles or microemulsions, the P-μE are quite stable to dilution, and remain intact over a wide range of concentrations. These properties are established by using photophysical properties of guest molecules in the systems. The P-μE exhibit two distinct sites of solubilization for a guest molecule: one in the surfactant coating and the second in the polymerized styrene core of the particle. The guest molecules are bound much more strongly to P-μE than to micelles. The two sites of guest solubilization in P-μE lead to unique effects on the quenching reactions involving excited guest and a quencher. For example, the excited guest molecules in the surfactant region are readily quenched by I^- or O_2, while those in the polymer are relatively unaffected. These systems provide vehicles for studying photoinduced reactions over controlled separation distances where the effects of diffusion are minimized.

Introduction

The past decade has seen considerable interest in the use of organized assemblies, i.e., micelles, microemulsions, vesicles, etc., to influence radiation-induced reactions.[2-5] A most useful extension of the work lies in the use of cross-linked polymerized assemblies,[6,7] in particular as applied to vesicular systems. Polymerization lends stability and permanence to these kinetic structures and secures solubilized moelcules more tightly.

(1) We wish to thank the NSF for support of this work (Grant CHE 24867).
(2) J. Fendler, *Acc. Chem. Res.*, **9**, 1953 (1976).
(3) N. Turro, M. Grätzel, and A. Braun, *Angew. Chem.*, **19**, 675 (1980).
(4) J. K. Thomas, *Chem. Rev.*, **80**, 283 (1980).
(5) T. S. Chen and J. K. Thomas, *J. Chem. Educ.*, **58**, 140 (1981).
(6) See *Chem. Eng. News.*, **59** (Aug 3), 8 (1981).
(7) L. Gras, H. Ringsdorf, and H. Schupp, *Angew. Chem., Int. Ed. Engl.*, **20**, 305 (1981).

0002-7863/82/1504-5868$01.25/0